Int. J. Solids Structures Vol. 30, No. 16, pp. 2199–2211, 1993
Printed in Great Britain

0020-7683/93 $6.00+ .00

VISCOELASTIC ANALYSIS OF BONDED TUBULAR JOINTS UNDER TORSION

HAIMING ZHOU and MOHAN D. RAO
Mechanical Engineering, Engineering Mechanics Department, Michigan Technological University, Houghton, MI 49931, U.S.A.

(*Received* 17 *August* 1992; *in revised form* 9 *March* 1993)

Abstract—In this paper, a theoretical analysis to evaluate the stress field in the adhesive layers of tubular bonded joints subjected to torsional loading is presented. The formulation is suitable to study the static behavior of the joint under general loading conditions as well as steady-state behavior under cyclic loading conditions. The adhesive material is modeled using linear viscoelasticity and numerical results for the shear stresses in the adhesives, joint compliance and joint loss factor are presented for various cases that provide some insights and guidelines in the design of the joint.

1. INTRODUCTION

Adhesively bonded joints have long been recognized as attractive alternatives to conventional mechanical joining techniques due to a greater uniformity in load distribution as well as reduced weight and processing ease. There is a need for a firm understanding of the nature of the stress and strain states that are found in adhesively bonded joints in order to effectively design these joints for a particular loading. There have been many types of adhesive bonded joints between tubes, but only a few analytical studies, mainly on single lap joints, have been reported in the literature. The stress analysis of tubular bonded joints is complicated because of the nonhomogeneous nature and the geometrical complexity of the medium, even for the case of joints made of linearly elastic materials. The existing works are based on certain simplifying assumptions with regard to the modeling of the adhesive and adherends. For the tubular lap joint analysis, Lubkin and Reissner (1956) considered the distribution of stress in the adhesive lap joint between thin cylindrical tubes of circular cross-section for the case in which the tubes are axially loaded. Alwar and Nagaraja (1976) solved the same problem by treating the adhesive material as viscoelastic material. Stresses in the tubular lap joint under torsional loading have been investigated by Adams and Peppiatt (1977). Chon (1982) has discussed the solution of the same problem when the adherends are composites. Medri (1988) recently gave a more comprehensive viscoelastic analysis of cemented lap joints subjected to torsion. Stresses in tubular lap joints under other loading conditions, such as external and internal pressures, have been investigated by Terekhova and Skoryi (1973). The tubular joint, however, is most often used under torsional loading, compared with other loadings, so the mechanical behavior under the torsional loading is very important.

The single lap joint is not a very efficient joint especially under torsional loading. A modified version that utilizes two layers of adhesives as shown in Fig. 1(a) is more attractive for many structural applications. This joint will be referred to here as a Tenon–Mortise type joint for tubular members. The joint is formed by cutting a projecting member (Tenon) in one tube and bonding it by insertion into the other tube (Mortise). The objective of this paper is to extend Medri's work to investigate the stress field, joint compliance and joint loss factor for the Tenon and Mortise type tubular joint under torsional loading. This type of joint has not been studied before to the best of the authors' knowledge. A theoretical model to evaluate the stress field in the adhesive layers and the joint compliance is presented. This problem is mathematically more complicated than the case of single lap joint presented by Medri (1988) because of the existence of two adhesive layers and the complexity of boundary conditions. Equations for shear stresses in the two adhesive layers are developed for the case of elastic, and viscoelastic adhesives under static loading. The study has been extended to include the quasi-static case and expressions for joint compliance and loss

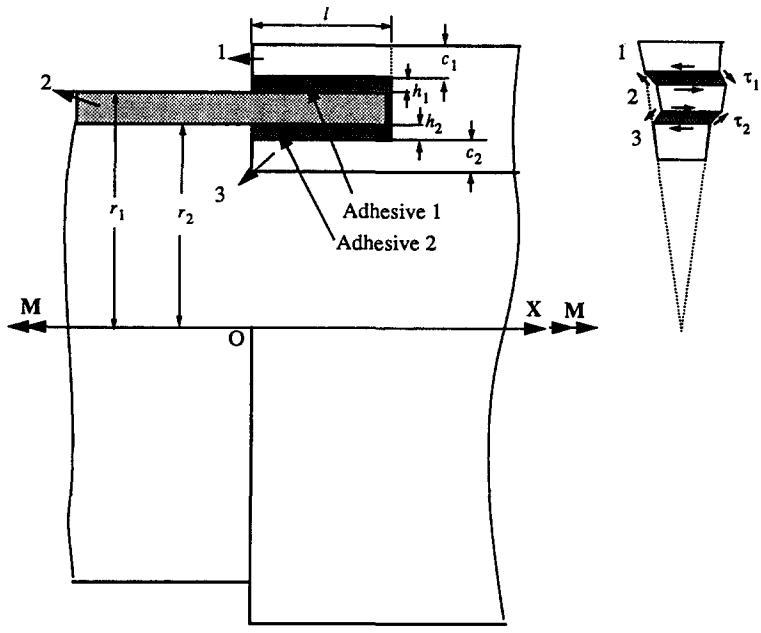

(a) Joint Configuration

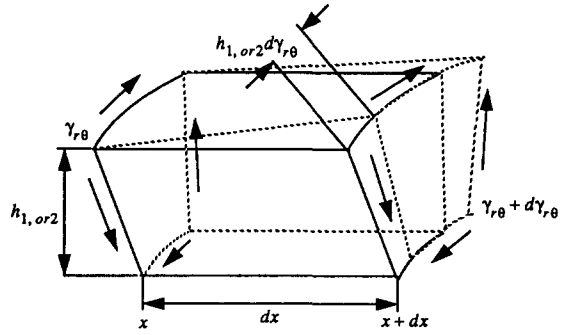

(b) The deformation of an arbitrary differential segment in the adhesive layer

Fig. 1. Bonded tubular lap joint.

factor (damping) are also developed. Some numerical results are generated for all of the above cases that are useful in the design of the joint.

2. THEORETICAL MODEL

A cylindrical coordinate system is chosen with the origin O fixed in tube 2 (Tenon) and placed at the left-hand end of the tube 1 (Mortise) as can be seen in Fig. 1(a). The principal assumptions are similar to the ones used by Medri (1988):

(1) The tubes are perfectly coaxial.
(2) The tubes are made of isotropic linear elastic materials.
(3) The tubes have perfectly circular cross-sections.
(4) The adhesive layer can be modeled as a linear viscoelastic material.
(5) The thickness of the adhesive layer is negligible with respect to the joint size.
(6) The problem can be studied using a quasi-static loading, i.e. neglect the inertia effects of both the tubes and the adhesive layer, assuming that very large inertial elements are connected to the tubes.
(7) Only the shear stress $\tau_{r\theta}$ in the adhesive (considered constant over the film thickness) and $\tau_{\theta x}$ in the tubes are taken into account. The remaining components of the

stress tensor in the tubes and in the adhesive layers are assumed to have negligible effects on joint deformation when a torque is applied to the tubes. The validity of this assumption has been proved earlier for single lap joints by Medri (1988).

From the above assumptions and kinematic considerations of a joint element of length dx [Fig. 1(b)] and balance of moments applied to the adherends, we can write:

$$h_1 d\gamma_1 = r_1\left(\frac{M_1}{D_1} - \frac{M_2}{D_2}\right)dx, \tag{1}$$

$$h_2 d\gamma_2 = r_2\left(\frac{M_3}{D_3} - \frac{M_2}{D_2}\right)dx, \tag{2}$$

$$M_1 + M_2 + M_3 = M, \tag{3}$$

$$M_1 = \int_0^x 2\pi r_1^2 \tau_1 \, d\xi, \tag{4}$$

$$M_3 = \int_0^x 2\pi r_2^2 \tau_2 \, d\xi. \tag{5}$$

The boundary conditions are:

$$\text{at } x = 0, \quad M_1 = M_3 = 0, \quad M_2 = M, \tag{6}$$

$$\text{at } x = l, \quad M_2 = 0, \quad M_1 + M_3 = M \quad \text{and} \quad \frac{M_1}{D_1} = \frac{M_3}{D_3}. \tag{7}$$

Here, M is the torque applied to the joint, M_1 is the portion of M acting on part 1 of the cross-section of the tube (Mortise), M_3 is the same on part 3, M_2 is the portion of torque M acting on the cross-section of tube 2 (Tenon). The shear stresses τ_1 and τ_2 are the $\tau_{r\theta}$ shear stresses in the outer and inner adhesive layers respectively, the shear strains γ_1 and γ_2 are the corresponding $\gamma_{r\theta}$ strains. Additionally, r_1 and r_2 are the outer and inner radii of tube 2, h_1 and h_2 are the thicknesses of outer and inner adhesive layers respectively and l is the overlap length. The term D_2 is the torsional stiffness of the tube as Tenon, D_1 and D_3 are the torsional stiffnesses in parts 1 and 3 of tube 1 as Mortise.

Substituting eqns (4) and (5) in eqn (3) yields

$$M_2 = M - M_1 - M_3 = M - \int_0^x 2\pi r_1^2 \tau_1 \, d\xi - \int_0^x 2\pi r_2^2 \tau_2 \, d\xi. \tag{8}$$

Substituting eqns (4) and (8) in eqn (1) and carrying out the differentiations with respect to x (denoted by prime), we have

$$\gamma_1'' = \frac{2\pi r_1^3}{h_1}\left(\frac{D_1 + D_2}{D_1 D_2}\right)\tau_1 + \frac{2\pi r_2^2 r_1}{h_1 D_2}\tau_2. \tag{9}$$

Similarly substituting eqns (5) and (8) in eqn (2) and differentiating it we have

$$\gamma_2'' = \frac{2\pi r_1^2 r_2}{h_2 D_2}\tau_1 + \frac{2\pi r_2^3}{h_2}\left(\frac{D_1+D_3}{D_2 D_3}\right)\tau_2. \tag{10}$$

2.1. *Elastic solution*

First we consider this problem as an elastic problem. For the adhesive material, we have $\tau = G\gamma$ where G is the shear modulus of the adhesive material. This gives $\gamma_1'' = (1/G)\tau_1''$, $\gamma_2'' = (1/G)\tau_2''$ and eqns (9) and (10), become

$$\tau_1'' = G\frac{2\pi r_1^3(D_1+D_2)}{h_1 D_1 D_2}\tau_1 + G\frac{2\pi r_1 r_2^2}{h_1 D_2}\tau_2 = GK_1\tau_1 + GK_2\tau_2, \tag{11}$$

$$\tau_2'' = G\frac{2\pi r_1^2 r_2}{h_2 D_2}\tau_1 + G\frac{2\pi r_2^3(D_3+D_2)}{h_2 D_3 D_2}\tau_2 = GK_3\tau_1 + GK_4\tau_2, \tag{12}$$

here, K_1, K_2, K_3 and K_4 are only related to the geometry and material parameters of Tenon and Mortise. From the above equations, after elimination of one of the variables, we have

$$\tau_2^{(4)} - G(K_1+K_4)\tau_2'' + G^2(K_1K_4 - K_2K_3)\tau_2 = 0. \tag{13}$$

A similar differential equation for τ_1 can also be obtained. The characteristic equation corresponding to eqn (13) is

$$\lambda^4 - G(K_1+K_4)\lambda^2 + G^2(K_1K_4 - K_2K_3) = 0. \tag{14}$$

The roots of the above equation are given by: $\lambda_{1,2} = (\pm G^{1/2})\alpha$, and $\lambda_{3,4} = (\pm G^{1/2})\beta$ where

$$\alpha = (\tfrac{1}{2}(K_1+K_4) + \tfrac{1}{2}((K_1+K_4)^2 - 4(K_1K_4 - K_2K_3))^{1/2})^{1/2}$$

and

$$\beta = (\tfrac{1}{2}(K_1+K_4) - \tfrac{1}{2}((K_1+K_4)^2 - 4(K_1K_4 - K_2K_3))^{1/2})^{1/2}. \tag{15}$$

The solutions for the shear stresses are:

$$\tau_1 = (c_1\sinh(\sqrt{G}\alpha x) + c_2\cosh(\sqrt{G}\alpha x) + c_3\sinh(\sqrt{G}\beta x) + c_4\cosh(\sqrt{G}\beta x))M \tag{16}$$

and

$$\tau_2 = (c_1'\sinh(\sqrt{G}\alpha x) + c_2'\cosh(\sqrt{G}\alpha x) + c_3'\sinh(\sqrt{G}\beta x) + c_4'\cosh(\sqrt{G}\beta x))M. \tag{17}$$

The constants c_i and c_i' ($i = 1, 2, 3, 4$) can be determined from boundary conditions given in eqns (6) and (7). After applying the boundary conditions, and solving for all of the unknown constants we get the elastic solutions of τ_1 and τ_2 as the following:

$$\begin{aligned}\tau_1 = {} & \frac{\sqrt{G}M}{D_2\alpha(\beta^2-\alpha^2)}\left(\frac{r_1K_1}{h_1} + \frac{r_2K_2}{h_2} - \frac{r_1\beta^2}{h_1}\right)\sinh(\sqrt{G}\alpha x) \\ & - \frac{\sqrt{G}M}{D_2\alpha(\beta^2-\alpha^2)}\left(\frac{r_1K_1}{h_1} + \frac{r_2K_2}{h_2} - \frac{r_1\beta^2}{h_1}\right) \\ & \times\left(\frac{\cosh(\sqrt{G}\alpha l)}{\sinh(\sqrt{G}\alpha l)} + \frac{D_2}{D_1+D_3}\frac{1}{\sinh(\sqrt{G}\alpha l)}\right)\cosh(\sqrt{G}\alpha x) \\ & + \frac{\sqrt{G}M}{D_2\beta(\alpha^2-\beta^2)}\left(\frac{r_1K_1}{h_1} + \frac{r_2K_2}{h_2} - \frac{r_1\alpha^2}{h_1}\right)\sinh(\sqrt{G}\beta x)\end{aligned}$$

$$-\frac{\sqrt{G}M}{D_2\beta(\alpha^2-\beta^2)}\left(\frac{r_1K_1}{h_1}+\frac{r_2K_2}{h_2}-\frac{r_1\alpha^2}{h_1}\right)$$

$$\times\left(\frac{\cosh(\sqrt{G}\beta l)}{\sinh(\sqrt{G}\beta l)}+\frac{D_2}{D_1+D_3}\frac{1}{\sinh(\sqrt{G}\beta l)}\right)\cosh(\sqrt{G}\beta x), \tag{18}$$

and

$$\tau_2=\frac{\sqrt{G}M(\alpha^2-K_1)}{D_2K_2\alpha(\beta^2-\alpha^2)}\left(\frac{r_1K_1}{h_1}+\frac{r_2K_2}{h_2}-\frac{r_1\beta^2}{h_1}\right)\sinh(\sqrt{G}\alpha x)-\frac{\sqrt{G}M(\alpha^2-K_1)}{D_2K_2\alpha(\beta^2-\alpha^2)}$$

$$\times\left(\frac{r_1K_1}{h_1}+\frac{r_2K_2}{h_2}-\frac{r_1\beta^2}{h_1}\right)\left(\frac{\cosh(\sqrt{G}\alpha l)}{\sinh(\sqrt{G}\alpha l)}+\frac{D_2}{D_1+D_3}\frac{1}{\sinh(\sqrt{G}\alpha l)}\right)\cosh(\sqrt{G}\alpha x)$$

$$+\frac{\sqrt{G}M(\beta^2-K_1)}{D_2K_2\beta(\alpha^2-\beta^2)}\left(\frac{r_1K_1}{h_1}+\frac{r_2K_2}{h_2}-\frac{r_1\alpha^2}{h_1}\right)\sinh(\sqrt{G}\beta x)-\frac{\sqrt{G}M(\beta^2-K_1)}{D_2K_2\beta(\alpha^2-\beta^2)}$$

$$\times\left(\frac{r_1K_1}{h_1}+\frac{r_2K_2}{h_2}-\frac{r_1\alpha^2}{h_1}\right)\left(\frac{\cosh(\sqrt{G}\beta l)}{\sinh(\sqrt{G}\beta l)}+\frac{D_2}{D_1+D_3}\frac{1}{\sinh(\sqrt{G}\beta l)}\right)\cosh(\sqrt{G}\beta x), \tag{19}$$

which describes the elastic stress field in the adhesives.

Defining $\tau_{av}=M/[2\pi(r_1^2+r_2^2)l]$, $K1(x)=(\tau_1/\tau_{av})$, $K2(x)=(\tau_2/\tau_{av})$ and considering the two tubes to be made of different materials, D_1 will be approximately equal to D_3, but D_2 will have a different magnitude compared with D_1 and D_3. Let $m=(G_T/G_M)$ be a nondimensional ratio of shear modulus of Tenon to Mortise tubes. Figures 2 and 3 show the variation of normalized adhesive shear stresses along the length of the bonded region. This result is generated for the case of $h_1=h_2=0.01$ m, $c_1=c_2=0.03$ m, $r_1=1.03$ m, $r_2=1$ m, $G=10^5$ Pa and $G_M=2.6\times10^9$ Pa. Figure 2 is plotted for the case where $m=1$, 10 and 100, i.e. the Tenon tube having stiffness equal to or greater than the Mortise tube, and Fig. 3 for $m=0.1$ and 0.01 in which the Tenon tube material is much softer compared with the Mortise tube. As seen, the maximum shear stress occurs at either end of the joint depending on the relative stiffness of the connecting members; it is at a maximum near the end of the stiffer tube. Furthermore, $K1$ appears to be greater than $K2$ for m greater than 1; they are almost equal when m takes on values less than 1. For m less than 1, from Fig. 3, it is evident that the joint is most likely to fail at the left-hand end. It is also seen that the stress concentration factor takes on a very high value (almost equal to 20) for the case of $m=0.01$. Figure 4 shows the results of maximum stress concentration factors (maximum

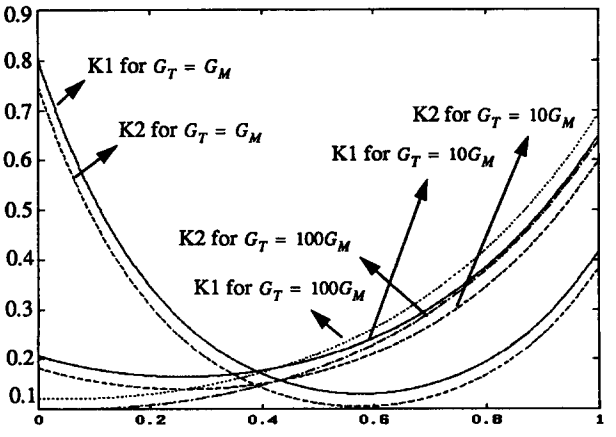

Fig. 2. Stress concentration factors $K1$, $K2$ versus coordinate x for $G_T/G_M=1$, 10, 100 and $G_M=2.6$ GPa.

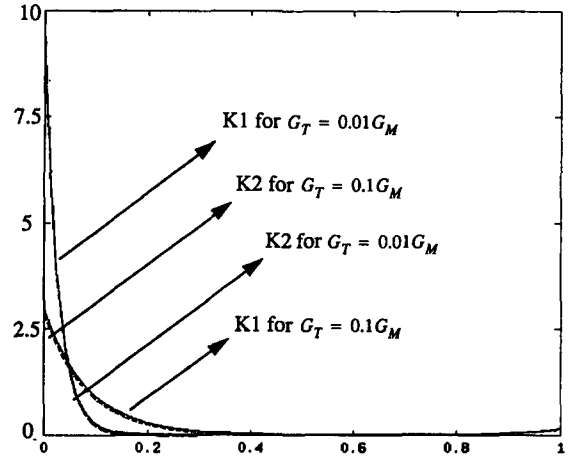

Fig. 3. Stress concentration factors $K1$, $K2$ versus coordinate x for $G_T/G_M = 0.1, 0.01$ and $G_M = 2.6$ GPa.

$K1$ and $K2$) as a function of the ratio m. It is clear from this figure that the stress concentration is maximum when the material of the tenon is very soft compared to the material of the Mortise tube. When the ratio of the stiffness of the two materials is greater than about 2, the stress concentration factor is almost constant. From the above figures, it can be concluded that while fabricating a joint of this type using two different adherends, it is always advantageous to choose the stiffer of the two as the Tenon material. Figure 5 shows the relationship between stress concentration factors (maximum $K1$ and $K2$) and the aspect ratio l/r_2. It is clear from this figure that an increase in the l/r_2 ratio beyond unity would lead to a significant increase in the stress levels.

It should be noted that the actual stress–strain fields at the roots of elements 1 and 3 are more complex because of the geometry selected and more refined analysis such as finite element analysis need to be employed to evaluate the complex stress–strain fields at these locations. It has been demonstrated, however, that the present analysis can indeed be used to predict both qualitatively and quantitatively the presence of stress concentration at these locations. Further work is currently in progress to compare the present results with FEM and experimental results, the results of which will be the subject of a future paper.

2.2. *Viscoelastic solution*

If a viscoelastic model is utilized to describe the mechanical behavior of the adhesive, the corresponding constitutive equation is (Flugge, 1975):

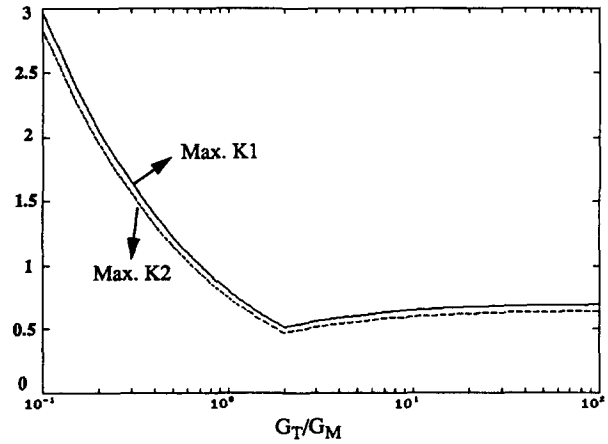

Fig. 4. Maximum $K1$ and $K2$ versus G_T/G_M for $G = 1.0$ MPa.

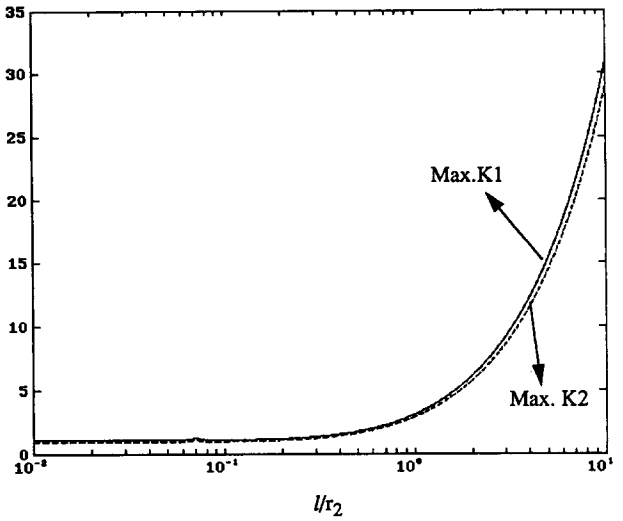

Fig. 5. Maximum $K1$ and $K2$ versus l/r_2 for $G_T = G_M = 100G = 2.6$ GPa.

$$P\tau = Q\gamma, \tag{20}$$

where P and Q are the classical linear differential operators of the viscoelastic laws. Then eqns (9) and (10) become

$$P\tau_1'' = K_1 Q\tau_1 + K_2 Q\tau_2, \tag{21}$$

$$P\tau_2'' = K_3 Q\tau_1 + K_4 Q\tau_2. \tag{22}$$

After eliminating τ_2 from eqn (22) we get an equation for τ_1:

$$PP\tau_1^{(4)} - (K_1 + K_4)PQ\tau_1'' + (K_1K_4 - K_2K_3)QQ\tau_1 = 0. \tag{23}$$

Similarly, τ_2 will also satisfy this equation.

Equation (23) above is a $(2n+4)$th order, linear, nonhomogeneous partial differential equation with constant coefficients in $\tau_1(x, t)$ and $\tau_2(x, t)$, n being the order of the P operator. The solution can be written as

$$\tau_1 = \sum_{j=1}^{\infty} c_j \, e^{(a_j x + b_j t)}, \quad \text{and} \quad \tau_2 = \sum_{j=1}^{\infty} c_j' \, e^{(a_j' x + b_j t)}. \tag{24}$$

The constants a_j, a_j' and b_j are related by the equations which are obtained by inserting eqn (24) into eqn (23):

$$a_j^4 - G(b_j)(K_1 + K_4)a_j^2 + G^2(b_j)(K_1K_4 - K_2K_3) = 0, \tag{25}$$

$$a_j'^4 - G(b_j)(K_1 + K_4)a_j'^2 + G^2(b_j)(K_1K_4 - K_2K_3) = 0, \tag{26}$$

where $G(i\omega)$ is the complex modulus of the adhesive. It can be expressed in the form $G(i\omega) = G(\omega)(1 + i\eta(\omega))$, where $G(\omega)$ is the real part of the complex modulus commonly referred as the storage modulus, and $\eta(\omega)$ is the loss factor of the adhesive material, both are functions of frequency.

With regard to the boundary conditions we can find two boundary conditions in the spatial coordinate x, and m initial conditions in time t (m is the order of the Q operator).

The boundary conditions in x are [for instance, with reference to Fig. 1 and eqns (1), (2), (6), (7)]:

$$P\tau_1' = -\frac{r_1}{h_1 D_2} QM(t) \quad \text{for } x = 0, \tag{27}$$

$$P\tau_2' = -\frac{r_2}{h_2 D_2} QM(t) \quad \text{for } x = 0, \tag{28}$$

$$P\tau_1' = \frac{r_1}{h_1(D_1+D_3)} QM(t) \quad \text{for } x = l, \tag{29}$$

$$P\tau_2' = \frac{r_2}{h_2(D_1+D_3)} QM(t) \quad \text{for } x = l. \tag{30}$$

The actual evaluation of the constants b_j, a_j, a_j', c_j, c_j' depends on the number of terms chosen in the viscoelastic constitutive equation. This will have to be performed by means of a nonlinear least-square method operating on the boundary equations and initial conditions.

2.3. *Joint compliance*

The angular rotation of the cross-section of the joint is valuable information which can be used in the design of the joint to guard against high deformations just as data on stress concentration are useful to predict joint failure. The normalized angular deformation is referred to here as joint compliance.

Let θ_1, be the rotation between the cross-sections of the tenon at $x = 0$ and part 1, and θ_2 be the rotation of the cross-section of the mortise for $x = l$ and part 3. The following equations are true:

$$\theta_1 = \frac{\gamma_{01} h_1}{r_1} + \int_0^l \frac{M_1}{D_1} dx = \frac{\gamma_{01} h_1}{r_1} + \int_0^l dx \int_0^x \frac{2\pi r_1^2}{D_1} \tau_1 \, d\xi, \tag{31}$$

$$\theta_2 = \frac{\gamma_{02} h_2}{r_2} + \int_0^l \frac{M_3}{D_3} dx = \frac{\gamma_{02} h_2}{r_2} + \int_0^l dx \int_0^x \frac{2\pi r_2^2}{D_3} \tau_2 \, d\xi, \tag{32}$$

where γ_{01} and γ_{02} are the shear strains in the two adhesive layers at $x = 0$.

Applying the Q operator to eqns (31) and (32) we get

$$Q\theta_1 = \frac{h_1}{r_1} P\tau_{01} + \frac{2\pi r_1^2}{D_1} \int_0^l dx \int_0^x Q\tau_1 \, d\xi = \sum_{j=1}^{\infty} A_j c_j \, e^{b_j t}, \tag{33}$$

$$Q\theta_2 = \frac{h_2}{r_2} P\tau_{02} + \frac{2\pi r_2^2}{D_3} \int_0^l dx \int_0^x Q\tau_2 \, d\xi = \sum_{j=1}^{\infty} A_j' c_j' \, e^{b_j t}, \tag{34}$$

in which

$$A_j = 2\pi r_1^2 (e^{a_j l} - a_j l - l) Q(b_j)/(a_j^2 D_1) + h_1 P(b_j)/r_1, \tag{35}$$

$$A_j' = 2\pi r_2^2 (e^{a_j' l} - a_j' l - l) Q(b_j)/(a_j'^2 D_3) + h_2 P(b_j)/r_1, \tag{36}$$

here $P(s)$ and $Q(s)$ are the Laplace transforms of P and Q. Finally one can write, for the general case,

$$\theta_1 = L^{-1}\left[\frac{\left(\sum_{j=1}^{\infty} A_j c_j/(s-b_j) + \sum_{k=0}^{m-1}\frac{\partial^k}{\partial t^k}\theta(0)\left(\sum_{i=k+1}^{m} q_i s^{i-k-1}\right)\right)}{Q(s)}\right], \tag{37}$$

$$\theta_2 = L^{-1}\left[\frac{\left(\sum_{j=1}^{\infty} A'_j c'_j/(s-b_j) + \sum_{k=0}^{m-1}\frac{\partial^k}{\partial t^k}\theta(0)\left(\sum_{i=k+1}^{m} q_i s^{i-k-1}\right)\right)}{Q(s)}\right]. \tag{38}$$

Within the elastic assumption, θ_1 and θ_2 can be determined by substituting the previously derived elastic expression of τ_1 and τ_2 into the above expression, and after some mathematical manipulation, we get

$$\theta_1 = \left(\frac{2\pi r_1^2}{D_1}\left(\frac{\sinh(\sqrt{G}\alpha l)-\sqrt{G}\alpha l}{G\alpha^2}c_1 + \frac{\cosh(\sqrt{G}\alpha l)-1}{G\alpha^2}c_2 + \frac{\sinh(\sqrt{G}\beta l)-\sqrt{G}\beta l}{G\beta^2}c_3 + \frac{\cosh(\sqrt{G}\beta l)-1}{G\beta^2}c_4\right) + \frac{(c_2+c_4)h_1}{Gr_1}\right)M \tag{39}$$

and

$$\theta_2 = \left(\frac{2\pi r_2^2}{D_3}\left(\frac{\sinh(\sqrt{G}\alpha l)-\sqrt{G}\alpha l}{G\alpha^2}c'_1 + \frac{\cosh(\sqrt{G}\alpha l)-1}{G\alpha^2}c'_2 + \frac{\sinh(\sqrt{G}\beta l)-\sqrt{G}\beta l}{G\beta^2}c'_3 + \frac{\cosh(\sqrt{G}\beta l)-1}{G\beta^2}c'_4\right) + \frac{(c'_2+c'_4)h_2}{Gr_2}\right)M. \tag{40}$$

Figure 6 shows the influence of the adhesive shear modulus (plotted as a ratio G/G_M) on θ_1 and θ_2. Here θ_1 and θ_2 are normalized as $\overline{\theta_1} = \theta_1/(Ml/D_2)$, $\overline{\theta_2} = \theta_2/(Ml/D_2)$. It is seen that the joint compliance decreases with an increase in the shear modulus of the adhesive. A similar trend is noticed for the variation of θ_1 and θ_2 with respect to the aspect ratio l/r_2

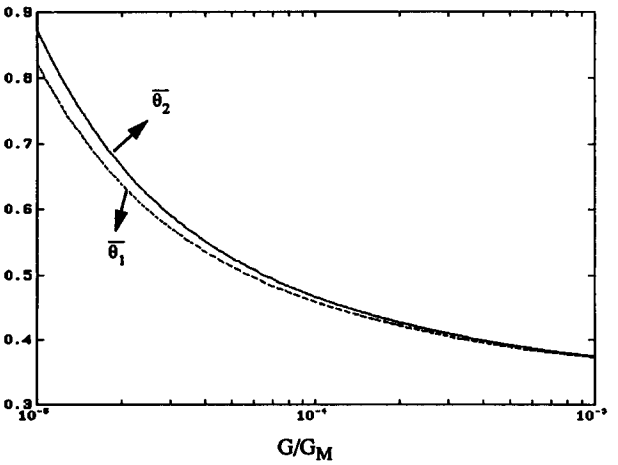

Fig. 6. Normalized $\overline{\theta_1}$, $\overline{\theta_2}$ versus G/G_M for constant l and $G_T = G_M = 2.6$ GPa.

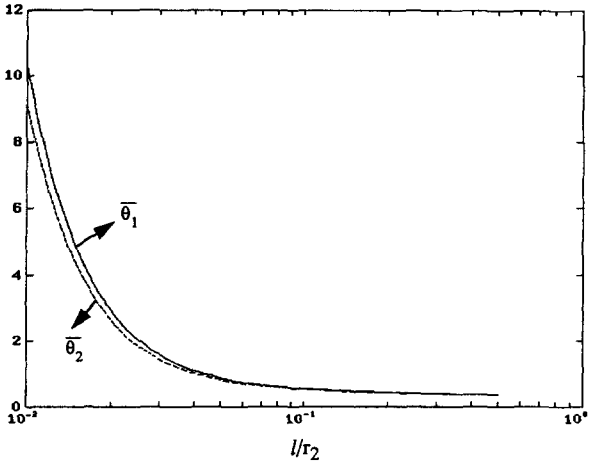

Fig. 7. Normalized $\overline{\theta_1}$, $\overline{\theta_2}$ versus l/r_2 for $G_T = G_M = 100G = 2.6$ GPa.

as seen in Fig. 7, the joint deformations are constant for aspect ratio greater than about 0.1. This implies there exists an optimum value of aspect ratio that needs to be chosen to guard against large deformations in the design of these joints. Figures 8 and 9 show 3-D plots of variation of joint compliance with respect to normalized adhesive shear modulus and joint aspect ratio.

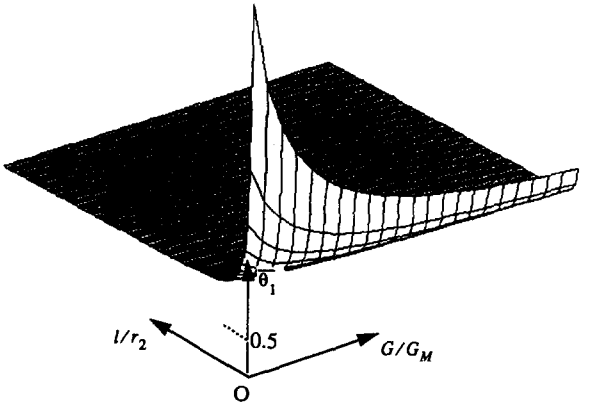

Fig. 8. Normalized $\overline{\theta_1}$ versus G/G_M and l/r_2.

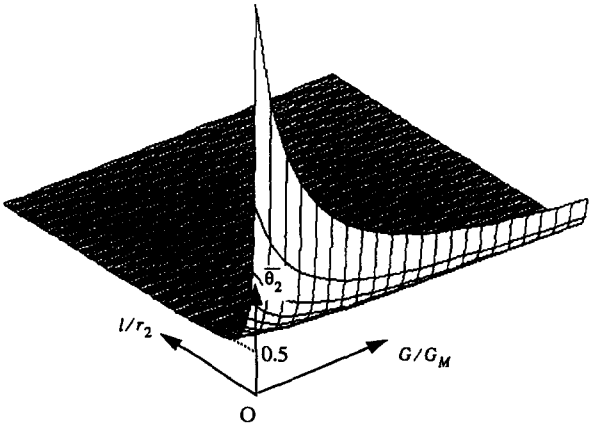

Fig. 9. Normalized $\overline{\theta_2}$ versus G/G_M and l/r_2.

2.4. *Quasi-static solution*

Finally, the solution for the adhesive shear stresses and joint compliance are discussed in this section for the case of steady-state oscillating torque of the form $M = M_0 e^{i\omega t}$, acting on the system. Here the use of the complex number description is more convenient. Denoting the complex compliance as $J_1(i\omega)$, $J_2(i\omega)$, we have

$$\theta_1 = J_1(i\omega) M_0 e^{i\omega t}, \tag{41}$$

$$\theta_2 = J_2(i\omega) M_0 e^{i\omega t}. \tag{42}$$

Applying the Q operator to the above equations as before we get,

$$Q\theta_1 = J_1(i\omega) Q(i\omega) M_0 e^{i\omega t}, \tag{43}$$

$$Q\theta_2 = J_2(i\omega) Q(i\omega) M_0 e^{i\omega t}. \tag{44}$$

For the general case, comparing eqns (33) and (34) with eqns (43) and (44), the complex compliance terms can be found easily. The adhesive shear stresses can be determined by setting the τ_1, τ_2 to be the same as in eqn (24), and combining suitable boundary conditions. For instance, suppose for $j = 1,\ldots,4$; $b_1 = b_2 = b_3 = b_4 = i\omega$; $a_1 = -a_2 = \sqrt{G(i\omega)}\alpha$; $a_3 = -a_4 = \sqrt{G(i\omega)}\beta$, using the boundary conditions of Fig. 1 we can eventually obtain the following result:

$$\begin{aligned}
\tau_1 = {} & \frac{\sqrt{G(i\omega)} M_0 e^{i\omega t}}{D_2\alpha(\beta^2-\alpha^2)}\left(\frac{r_1K_1}{h_1}+\frac{r_2K_2}{h_2}-\frac{r_1\beta^2}{h_1}\right)\sinh(\sqrt{G(i\omega)}\alpha x)-\left(\frac{r_1K_1}{h_1}+\frac{r_2K_2}{h_2}-\frac{r_1\beta^2}{h_1}\right)\\
& \times\frac{\sqrt{G(i\omega)} M_0 e^{i\omega t}}{D_2\alpha(\beta^2-\alpha^2)}\left(\frac{\cosh(\sqrt{G(i\omega)}\alpha l)}{\sinh\sqrt{G(i\omega)}\alpha l)}+\frac{D_2}{D_1+D_3}\frac{1}{\sinh(\sqrt{G(i\omega)}\alpha l)}\right)\cosh(\sqrt{G(i\omega)}\alpha x)\\
& +\frac{\sqrt{G(i\omega)} M_0 e^{i\omega t}}{D_2\beta(\alpha^2-\beta^2)}\left(\frac{r_1K_1}{h_1}+\frac{r_2K_2}{h_2}-\frac{r_1\alpha^2}{h_1}\right)\sinh(\sqrt{G(i\omega)}\beta x)-\left(\frac{r_1K_1}{h_1}+\frac{r_2K_2}{h_2}-\frac{r_1\alpha^2}{h_1}\right)\\
& \times\frac{\sqrt{G(i\omega)} M_0 e^{i\omega t}}{D_2\beta(\alpha^2-\beta^2)}\left(\frac{\cosh(\sqrt{G(i\omega)}\beta l)}{\sinh(\sqrt{G(i\omega)}\beta l)}+\frac{D_2}{D_1+D_3}\frac{1}{\sinh(\sqrt{G(i\omega)}\beta l)}\right)\cosh(\sqrt{G(i\omega)}\beta x),
\end{aligned} \tag{45}$$

and

$$\begin{aligned}
\tau_2 = {} & \frac{\sqrt{G(i\omega)} M_0 e^{i\omega t}}{D_2K_2\alpha(\beta^2-\alpha^2)}\left(\frac{r_1K_1}{h_1}+\frac{r_2K_2}{h_2}-\frac{r_1\beta^2}{h_1}\right)\sinh(\sqrt{G(i\omega)}\alpha x)\\
& -\frac{\sqrt{G(i\omega)} M_0 e^{i\omega t}(\alpha^2-K_1)}{D_2K_2\alpha(\beta^2-\alpha^2)}\left(\frac{\cosh(\sqrt{G(i\omega)}\alpha l)}{\sinh(\sqrt{G(i\omega)}\alpha l)}+\frac{D_2}{D_1+D_3}\frac{1}{\sinh(\sqrt{G(i\omega)}\alpha l)}\right)\\
& \times\left(\frac{r_1K_1}{h_1}+\frac{r_2K_2}{h_2}-\frac{r_1\beta^2}{h_1}\right)\cosh(\sqrt{G(i\omega)}\alpha x)\\
& +\frac{(\sqrt{G(i\omega)} M_0 e^{i\omega t}(\beta^2-K_1)}{D_2K_2\beta(\alpha^2-\beta^2)}\left(\frac{r_1K_1}{h_1}+\frac{r_2K_2}{h_2}-\frac{r_1\alpha^2}{h_1}\right)\\
& \times\sinh(\sqrt{G(i\omega)}\beta x)-\frac{(\sqrt{G(i\omega)} M_0 e^{i\omega t}(\beta^2-K_1)}{D_2K_2\beta(\alpha^2-\beta^2)}\left(\frac{r_1K_1}{h_1}+\frac{r_2K_2}{h_2}-\frac{r_1\alpha^2}{h_1}\right)\\
& \times\left(\frac{\cosh(\sqrt{G(i\omega)}\beta l)}{\sinh(\sqrt{G(i\omega)}\beta l)}+\frac{D_2}{D_1+D_3}\frac{1}{\sinh(\sqrt{G(i\omega)}\beta l)}\right)(\cosh(\sqrt{G(i\omega)}\beta x)).
\end{aligned} \tag{46}$$

Here $G(i\omega) = P(i\omega)/Q(i\omega) = G_r(\omega)(1+i\eta_m(\omega))$. It should be noted again that $G_r(\omega)$ is the real part of the complex modulus of the adhesive materials, commonly referred to as the storage modulus, and $\eta_m(\omega)$ is the loss factor of the adhesive material.

Combining eqns (33), (34) (in which set $b_j = i\omega$), and eqns (43)–(46), we also get

$$
\begin{aligned}
J_1(i\omega) = {} & \left(\frac{(\sqrt{G(i\omega)}}{D_2\alpha(\beta^2-\alpha^2)}\left(\frac{r_1K_1}{h_1}+\frac{r_2K_2}{h_2}-\frac{r_1\beta^2}{h_1}\right)\frac{(\sinh(\sqrt{G(i\omega)}\alpha l)-(\sqrt{G(i\omega)}\alpha l)}{G(i\omega)\alpha^2}\frac{2\pi r_1^2}{D_1}\right.\\
& -\frac{(\sqrt{G(i\omega)}}{D_2\alpha(\beta^2-\alpha^2)}\left(\frac{r_1K_1}{h_1}+\frac{r_2K_2}{h_2}-\frac{r_1\beta^2}{h_1}\right)\left(\frac{\cosh(\sqrt{G(i\omega)}\alpha l)}{\sinh(\sqrt{G(i\omega)}\alpha l)}+\frac{D_2}{D_1+D_3}\frac{1}{\sinh(\sqrt{G(i\omega)}\alpha l)}\right)\\
& \times\left(\frac{2\pi r_1^2(\cosh(\sqrt{G(i\omega)}\alpha l)-1)}{D_1G(i\omega)\alpha^2}+\frac{h_1}{G(i\omega)r_1}\right)+\left(\frac{r_1K_1}{h_1}+\frac{r_2K_2}{h_2}-\frac{r_1\alpha^2}{h_1}\right)\\
& \times\frac{\sinh(\sqrt{G(i\omega)}\beta l)-(\sqrt{G(i\omega)}\beta l}{G(i\omega)\beta^2}\frac{(\sqrt{G(i\omega)}}{D_2\beta(\alpha^2-\beta^2)}\frac{2\pi r_1^2}{D_1}\\
& -\left(\frac{\cosh(\sqrt{G(i\omega)}\beta l)}{\sinh(\sqrt{G(i\omega)}\beta l)}+\frac{D_2}{D_1+D_3}\frac{1}{\sinh(\sqrt{G(i\omega)}\beta l)}\right)\frac{(\sqrt{G(i\omega)}}{D_2\beta(\alpha^2-\beta^2)}\\
& \left.\times\left(\frac{r_1K_1}{h_1}+\frac{r_2K_2}{h_2}-\frac{r_1\alpha^2}{h_1}\right)\left(\frac{2\pi r_1^2(\cosh(\sqrt{G(i\omega)}\beta l)-1)}{D_1G(i\omega)\beta^2}+\frac{h_1}{G(i\omega)r_1}\right)\right)M. \qquad (47)
\end{aligned}
$$

$$
\begin{aligned}
J_2(i\omega) = {} & \frac{(\sqrt{G(i\omega)}}{D_2\alpha(\beta^2-\alpha^2)}\left(\frac{\cosh(\sqrt{G(i\omega)}\alpha l)}{\sinh(\sqrt{G(i\omega)}\alpha l)}+\frac{D_2}{D_1+D_3}\frac{1}{\sinh(\sqrt{G(i\omega)}\alpha l)}\right)\frac{\alpha^2-K_1}{K_2}\\
& \times\left(\frac{r_1K_1}{h_1}+\frac{r_2K_2}{h_2}-\frac{r_1\beta^2}{h_1}\right)\frac{2\pi r_2^2}{D_3}-\frac{(\sqrt{G(i\omega)}}{D_2\alpha(\beta^2-\alpha^2)}\\
& \times\left(\frac{\cosh(\sqrt{G(i\omega)}\alpha l)}{\sinh(\sqrt{G(i\omega)}\alpha l)}+\frac{D_2}{D_1+D_3}\frac{1}{\sinh(\sqrt{G(i\omega)}\alpha l)}\right)\\
& \times\left(\frac{r_1K_1}{h_1}+\frac{r_2K_2}{h_2}-\frac{r_1\beta^2}{h_1}\right)\frac{\alpha^2-K_1}{K_2}\left(\frac{2\pi r_1^2(\cosh(\sqrt{G(i\omega)}\alpha l)-1)}{D_1G(i\omega)\alpha^2}\right.\\
& \left.+\frac{h_2}{G(i\omega)r_2}\right)\frac{2\pi r_2^2}{D_3}+\frac{(\sqrt{G(i\omega)}}{D_2\beta(\alpha^2-\beta^2)}\frac{\beta^2-K_1}{K_2}\left(\frac{r_1K_1}{h_1}+\frac{r_2K_2}{h_2}-\frac{r_1\alpha^2}{h_1}\right)\\
& \times\frac{(\sinh(\sqrt{G(i\omega)}\beta l)-(\sqrt{G(i\omega)}\beta l)}{G(i\omega)\beta^2}\frac{2\pi r_2^2}{D_3}-\frac{(\sqrt{G(i\omega)}}{D_2\beta(\alpha^2-\beta^2)}\\
& \times\left(\frac{\cosh(\sqrt{G(i\omega)}\beta l)}{\sinh(\sqrt{G(i\omega)}\beta l)}+\frac{D_2}{D_1+D_3}\frac{1}{\sinh(\sqrt{G(i\omega)}\beta l)}\right)\left(\frac{2\pi r_2^2(\cosh(\sqrt{G(i\omega)}\beta l)-1)}{D_3G(i\omega)\beta^2}+\frac{h_2}{G(i\omega)r_2}\right)\\
& \times\frac{\beta^2-K_1}{K_2}\left(\frac{r_1K_1}{h_1}+\frac{r_2K_2}{h_2}-\frac{r_1\alpha^2}{h_1}\right). \qquad (48)
\end{aligned}
$$

The terms $J_1(i\omega)$, $J_2(i\omega)$ are complex joint compliances which can be split into real and imaginary parts or magnitude and phase portions, the derivations of which are very complicated and lengthy. But it is not difficult to obtain the complex compliances in the form $J(i\omega) = J(1+i\eta)$ for computing numerical values using the above equations. The term η is referred to here as the joint loss factor which is essentially the phase difference between the torque and torsional deformation. Denoting the real and imaginary parts of $J_1(i\omega)$, $J_2(i\omega)$ as $\mathrm{Re}(J_1)$, $\mathrm{Im}(J_1)$, $\mathrm{Re}(J_2)$ and $\mathrm{Im}(J_2)$, we introduce two loss factor terms, $\eta_1 = -[\mathrm{Im}(J_1)/\mathrm{Re}(J_2)]$, and $\eta_2 = -[\mathrm{Im}(J_2)/\mathrm{Re}(J_2)]$. Figure 10 is a plot of these loss

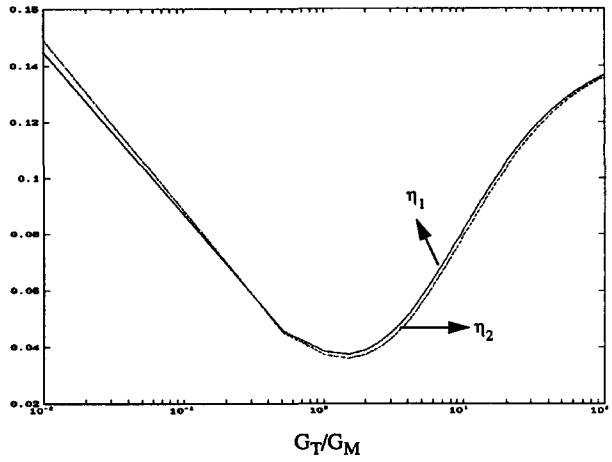

Fig. 10. Loss factors η_1, η_2 versus G_T/G_M for $G = 10^6$ (1+i0.3) Pa.

factors as a function of G_T/G_M for $G = 10^6(1+i0.3)$ Pa. From Fig. 10 we realize that η_1, η_2 are very close, but not the same, which is true because of our previous observation that θ_1, θ_2 are very close for a constant value of torque applied to the joint. Furthermore, we expect θ_1, θ_2 to be somewhat different because of the viscoelastic nature of the adhesive. Also, from Fig. 9, it is apparent that large phase difference, hence more energy dissipation occurs when the relative stiffness of the two adherends is either very large, or very small, i.e. at the extreme ends of Fig. 10. The joint loss factor for the case of same adherends is about 0.04 which is an order lower than the loss factor of the adhesive material used in the bonding of the joint. Finally, it is easy to show that, when $\omega \to 0$ then $G(i\omega) \to q_0$ and the quasi-static solution tends to the static solution, and the dynamic compliance tends to the static compliance.

3. CONCLUSIONS

A theoretical formulation to evaluate the shear stress field in the adhesives of a bonded Tenon–Mortise type tubular joint subjected to torsional loading is presented in this paper. The adhesive is modeled as a linear viscoelastic material and the adherends are assumed to be elastic. Equations for the adhesive shear stresses, and joint compliance are obtained for the case of static and steady oscillating torque applied to the joint. Furthermore, joint loss factor for the steady-state case has also been determined and all of the above results are plotted for various cases. It has been shown that the theoretical model, although a little bulky in mathematical expression, can be used to obtain some insights and guidelines in the design of such joints.

Acknowledgements—The authors would like to acknowledge the financial support provided by the National Science Foundation for support of this research through a research grant MSM-8910012 with Dr Ken P. Chong serving as the program director.

REFERENCES

Adams, R. D. and Peppiatt, N. A. (1977). Stress analysis of bonded tubular lap joints. *J. Adhesion* **9**, 1–18.
Alwar, R. S. and Nagaraja, Y. R. (1976). Viscoelastic analysis of an adhesive tubular joint. *J. Adhesion* **8**, 79–92.
Chon, C. T. (1982). Analysis of tubular lap joint in torsion. *J. Compos. Mater.* **16**, 268–283.
Flugge, W. (1975). *Viscoelasticity*. Springer, New York.
Lubkin, J. L. and Reissner, E. (1956). Stress distribution and design data for adhesive lap joints between circular tubes. *Trans. ASME* **78**, 1213–1221.
Medri, G. (1988). Viscoelastic analysis of adhesive bonded lap joints between tubes under torsion. *J. Vibr. Acoust. Stress Reliability Des.* **110**, 384–388.
Terekhova, L. P. and Skoryi, I. A. (1973). Stresses in bonded joints of thin cylindrical shells. *Strength Mater.* **4**, 1271–1274 (translated from Problemy Prochnosti **10**, 108–111, 1972).